35th Annual International Conference of the IEEE EMBS
Osaka, Japan, 3 - 7 July, 2013

An Automated Algorithm for Blood Vessel Count and Area Measurement in 2-D Choroidal Scan Images

Nagaraj R. Mahajan[1], Ravi Chandra Reddy Donapati[1], Sumohana S. Channappayya[1,*], *Member IEEE*, Sivaramakrishna Vanjari[1], Ashutosh Richhariya[2], Jay Chhablani[2]

***Abstract*— We present an automated algorithm for the detection of blood vessels in 2-D choroidal scan images followed by a measurement of the area of the vessels. The objective is to identify vessel parameters in the choroidal stroma that are affected by various abnormalities. The algorithm is divided into five stages. In the first stage, the image is denoised to remove sensor noise and facilitate further processing. In the second stage, the image is segmented in order to find the region of interest. In the third stage, three different contour detection methods are applied to address different challenges in vessel contour. In the fourth stage, the outputs of the three contour detection methods are combined to achieve refined vessel contour detection. In the fifth and final stage, the area of these contours are measured. The results have been evaluated by a practicing opthalmologist and performance of the algorithm relative to expert detection is reported.**

I. INTRODUCTION

The choroid acts as a connective tissue to the retina and sclera and supplies blood to these areas. It plays a crucial role in oxygenation and metabolic activity of the eye [1]. It has two parts i) Choriocapillaris ii) Choroidal stroma [2]. The choroidal stroma has blood vessels along with melanocytes, fibroblasts, immune cells, neurons, and ground substance. It is well known that the onset of disease or ageing changes the structure of the choroidal stroma, particularly vessel thickness and volume [3], [4]. To observe the changes in choroid with disease or ageing optical coherence tomography (OCT) imaging is considered as a useful tool [5], [6]. However, presence of speckles, low contrast and high absorption of light makes an OCT image difficult to understand [7]. Methods of characterization of choroidal structure are still being developed with several automated and manual image enhancement methods being proposed [8], [9]. The proposed algorithm is closest in its goal and philosophy to the work by Zhang et. al. [9]. However, in this paper, we work with 2-D images and address the challenges presented therein. We propose a new 2-D automated approach for evaluation of the choroidal vessels from the spectral domain (SD)-OCT images and compare the outcomes with manual outcomes for its reliability.

*This work is supported by the DIT, India under the Cyber Physical Systems Innovation Hub under Grant number: 13(6)/2010-CC&BT , Dated 01.03.11.

[1]Dept. of Electrical Engineering, Indian Institute of Technology Hyderabad, Yeddumailaram, AP - 502205, India (phone: +91 40 23017081, email: {EE09B040, EE90B028, sumohana, svanjari}@iith.ac.in).

[2]L. V. Prasad Eye Institute Hyderabad, AP - 500034, India (email: {ashutosh, jaychhablani}@lvpei.org).

The paper is organized as follows. Section II formulates the problem in terms of the challenges involved. Section III discusses the proposed algorithm in detail and results are presented in section IV. Section V concludes the paper and discusses directions for future work.

II. PROBLEM FORMULATION

As mentioned in section I, the primary goal of this work is to automatically detect and measure the size of blood vessels present below the choroid. The challenges involved are described in the following with the aid of a typical choroidal scan image acquired using OCT as shown in Fig. 1. Due to the nature of the acquisition process in OCT [10], noise is inherent to choroidal scan images. The presence of noise is detrimental to any automatic processing and its suppression is the first of the challenges. The choroidal layer has the most prominent intensity in the image and adversely affects enhancement of the vessel region. This is the second challenge to be addressed. The next task to be addressed is vessel contour detection. This is broken down into three sub-problems as follows. A careful observation of Fig. 1 reveals that the vessels can be located close to each other, have low intensity boundaries, and a few of them can have large areas. The first sub-problem is to detect and separate closely located vessels, the second sub-problem is to detect vessels with small area and the last one is to find the major vessels. The last challenge is to find the area of the vessel contours output by the solution to the previous step. Thus, we attempt to solve a series of five challenges as part of the proposed automated algorithm.

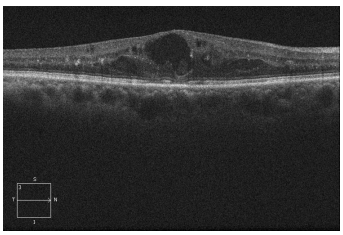

Fig. 1: Typical choroidal OCT scan image.

III. PROPOSED SOLUTION

The flowchart of the proposed algorithm is shown in Fig. 2. Each stage of the algorithm is discussed in the following.

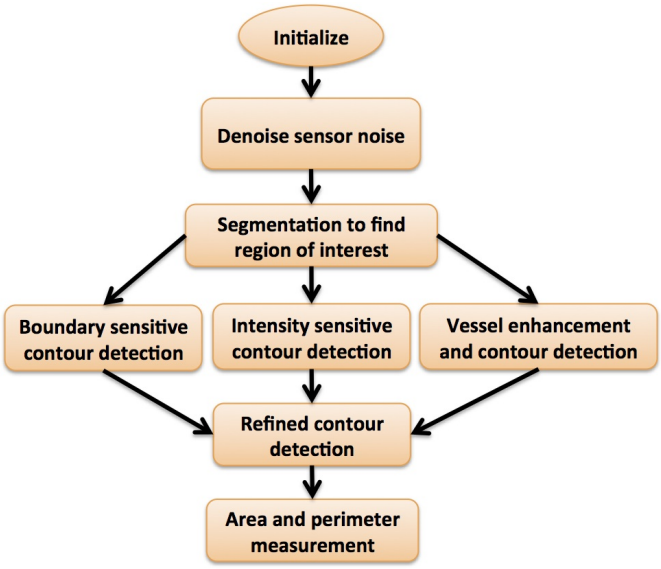

Fig. 2: Flowchart of proposed algorithm

A. Denoising

As shown in Fig. 1, a typical OCT scan image is inherently noisy [7]. Unlike other segmentation algorithms [9], [8], we first denoise the image to minimize its effect on subsequent stages in the proposed algorithm. This step is motivated by the fact that segmentation and detection algorithm almost always involves a differencing (gradient) operation. It is well known [11] that noise severely degrades the performance of gradient-based methods. Since denoising is only a means to the end goal, no attempt has been made to solve a denoising problem specific to OCT images. Instead, BM3D [12], a well-known image denoising algorithm was applied to denoise sensor noise. Noise standard deviation was empirically determined to be 25 and input to the denoising algorithm. We assume the noise to be additive, zero mean and white Gaussian. This assumption can be removed if a blind denoiser were used instead.

B. Segmentation

The next step in the algorithm is to segment the image so that the region of interest is not dominated by the high intensity choroid layer. This is achieved in a two step procedure. Population thresholding is first applied to the image to find the major edges in the image. In this method, an empirically chosen threshold of 150 is used to binarize the image. To eliminate noise, a majority filter is applied on the binarized image. The filter size is 5×5 and majority is considered to be 60%. To find the contour of the choroid, the mean location of the white pixels (or its center of mass) is found column wise. All pixels other than the mean location are set to black and the mean location is set to white. This gives an approximation of the choroid contour but is found to be noisy. A smooth estimate of the contour is found by polynomial curve fitting using a third order polynomial. Once this curve is found, all pixels located above it are set to black. This retains only the region of interest below the choroid and is better suited for enhancement and segmentation.

C. Three methods for contour detection

To address the three sub-problems mentioned in section II, the following solutions are proposed.

1) Boundary sensitive detection: Boundary sensitive detection is achieved using a combination of full scale contrast stretch (FSCS) and local thresholding. To achieve good boundary sensitivity it is important that even the faintest and most closely located edges are detected. Contrast enhancement is a pre-requisite to good edge detection. A sliding window FSCS is applied on the entire image with an empirically determined window size of 10×50. After this stage, the image is partitioned into non-overlapping blocks of size 150×150. Each block is binarized using a threshold set to its respective average.

2) Intensity sensitive detection: To achieve intensity sensitive contour detection a connected components-based algorithm [11] is proposed. The algorithm is based on the observation that there is a noticeable drop off in the pixel intensity beyond the vessel boundary. A simple analogy: assume that we want to count the number of branches in a dry tree and their height. Place the tree in a glass container and start to fill the container with water. At each water level, all un-submerged branches are counted. The number of branches that were previously not submerged but got submerged at the current level gives a count of the number of branches at that level. This method allows for the detection of small vessels as well and is outlined below.

Data: Segmented image
Result: Identify contours
Pick initial threshold T (average of bottom-left 20×50 patch) and binarize image;
Do connected components analysis to find blobs;
while *final threshold* T_f *(180, empirical) is not reached* **do**
    $T = T + \delta$ for empirically chosen δ;
    Compute connected components at new T;
    if a component disappears, detect it as a vessel
end

Algorithm 1: Intensity sensitive detection algorithm.

3) Vessel enhancement and detection: To achieve this goal, the popular technique proposed by Frangi et. al. [13] is applied to the segmented image output. In addition to vessel enhancement, it also does vessel detection. This technique clearly detects all the major vessel contours in the image albeit blurring the boundaries of closely located vessels.

D. Refined contour detection

The outputs of the methods described in section III-C are each designed to address a specific challenge. These outputs are combined in a way so as to retain the best features of each of them. The output of the boundary sensitive technique is logically ANDed with the output of the vessel enhancement

and detection stage. This achieves major vessel detection and good boundary separation of closely located vessels. This output is then logically ORed with the output of the intensity sensitive stage and connected components analysis is done to give the refined output.

E. Area measurement

Once the refined contour detection is complete, a list of vessel contours along with labels are available. Area is computed by simply counting the number of pixels associated with each contour label.

IV. RESULTS

The output of each stage of the algorithm is shown in Fig. 3 and discussed in the following. The reference scan image is shown in Fig. 3(a). The result of denoising using the popular method by Dabov et. al. [12] is shown in Fig. 3(b). The denoised image is much better suited for gradient based operations than the reference. The result of population thresholding in shown in Fig. 3(c). This step clearly identifies the strong edges in the image which in this case happen to be the choroid. However, this image is noisy and doesn't present a clean boundary for segmentation. The output of white pixel location averaging is shown in Fig. 3(d). This is a clear improvement over the previous step but still noisy. To get a well defined boundary, a polynomial curve fit is done on the average output as shown in Fig. 3(e). This curve is used to segment the image and results in Fig. 3(f). At this point, three different contour detection methods are applied to account for the challenges involved. Fig. 3(g) is the output of the boundary sensitive detection method. Intensity sensitive detection result in shown in Fig. 3(h). The output of the popular vessel enhancement technique in [13] is shown in Fig. 3(i). The boundary sensitive and the Frangi method are combined to give improved boundary separation as seen in Fig. 3(j). This in turn is combined with the output of the intensity sensitive method to give the final vessel contour detection and is shown in Fig. 3(k). For comparison, the ground truth vessel detection done by an expert is shown in Fig. 3(l).

Statistical measures of performance for 12 images with ground truth data available is shown in Table I. Based on the false positive and false negative values, we see that the proposed method performs well over a range of images barring a few exceptions. A comparison of the areas reported by an expert and the proposed method for the image in Fig. 3(a) is shown in Table II. A comparison of area, the Hausdorff distance and mean absolute difference shows that the proposed algorithm correlates well with expert scores. We attribute this consistency to the systematic way in which the vessel contour detection problem was analysed and divided into sub-problems of boundary sensitive, intensity sensitive and vessel boundary enhanced detection. Each of these sub-problems was solved using an appropriate set of tools and the result of each stage combined to give a clean solution. The algorithm takes about 4.5 seconds per image on a laptop with Intel Core-i3 processor at 2.4 GHz and 4GB RAM.

Total vessels	False positives	False negatives
43	6	4
42	9	3
30	7	6
36	9	4
49	12	10
37	6	2
29	13	0
29	15	0
16	10	3
22	12	4
31	6	4
32	4	2

TABLE I: Classification statistics.

V. CONCLUSION AND FUTURE WORK

In this paper, we present a novel algorithm for the detection of blood vessel contours in 2D-OCT choroidal scan images and finding their area. The algorithm performed consistently over a wide range of images as verified statistically. It was observed that the performance of the proposed method can be improved in cases where the vessels are either closely located or sparse. Our future work would be directed towards improving the performance in these cases using inputs from expert opthalmologists.

REFERENCES

[1] D. Nickla and J. Wallman, "The multifunctional choroid," *Progress in retinal and eye research*, vol. 29, no. 2, pp. 144–168, 2010.

[2] M. Hogan, J. Alvarado, J. Weddell, *et al.*, *Histology of the human eye: an atlas and textbook*. Saunders Philadelphia, PA, 1971.

[3] R. Mullins, M. Johnson, E. Faidley, J. Skeie, and J. Huang, "Choriocapillaris vascular dropout related to density of drusen in human eyes with early age-related macular degeneration," *Investigative ophthalmology & visual science*, vol. 52, no. 3, pp. 1606–1612, 2011.

[4] D. McLeod, R. Grebe, I. Bhutto, C. Merges, T. Baba, and G. Lutty, "Relationship between rpe and choriocapillaris in age-related macular degeneration," *Investigative ophthalmology & visual science*, vol. 50, no. 10, pp. 4982–4991, 2009.

[5] S. Motaghiannezam, D. Koos, and S. Fraser, "Differential phase-contrast, swept-source optical coherence tomography at 1060 nm for in vivo human retinal and choroidal vasculature visualization," *Journal of Biomedical Optics*, vol. 17, no. 2, pp. 026011–1, 2012.

[6] T. Torzicky, "Retinal polarization-sensitive optical coherence tomography at 1060 nm with 350 khz a-scan rate using an fourier domain mode locked laser.," *Journal of Biomedical Optics*, vol. 18, no. 1, pp. 026011–1, 2013.

[7] A. Mishra, A. Wong, K. Bizheva, and D. Clausi, "Intra-retinal layer segmentation in optical coherence tomography images," *Optics express*, vol. 17, no. 26, pp. 23719–23728, 2009.

[8] E. Götzinger, M. Pircher, W. Geitzenauer, C. Ahlers, B. Baumann, S. Michels, U. Schmidt-Erfurth, and C. Hitzenberger, "Retinal pigment epithelium segmentation by polarization sensitive optical coherence tomography," *Optics express*, vol. 16, no. 21, pp. 16410–16422, 2008.

[9] L. Zhang, K. Lee, M. Niemeijer, R. Mullins, M. Sonka, and M. Abràmoff, "Automated segmentation of the choroid from clinical sd-oct," *Investigative Ophthalmology & Visual Science*, vol. 53, no. 12, pp. 7510–7519, 2012.

[10] J. Fujimoto, C. Pitris, S. Boppart, and M. Brezinski, "Optical coherence tomography: an emerging technology for biomedical imaging and optical biopsy," *Neoplasia (New York, NY)*, vol. 2, no. 1-2, p. 9, 2000.

[11] R. C. Gonzalez and R. E. Woods, *Digital Image Processing (3rd Edition)*. Prentice Hall, 2008.

[12] K. Dabov, A. Foi, V. Katkovnik, and K. Egiazarian, "Image denoising by sparse 3-d transform-domain collaborative filtering," *Image Processing, IEEE Transactions on*, vol. 16, no. 8, pp. 2080–2095, 2007.

[13] A. Frangi, W. Niessen, K. Vincken, and M. Viergever, "Multiscale vessel enhancement filtering," *Medical Image Computing and Computer-Assisted InterventationMICCAI98*, pp. 130–137, 1998.

Vessel index	Pixel area – algorithm	Pixel area – expert	Hausdorff distance	Mean absolute difference (MAD)
1	1026	1266	10.77	240
5	106	104	4.24	2
6	1222	1133	18	334
7	736	789	9.21	53
8	2193	3150	15	957
14	627	519	11.18	108
15	203	199	7.81	11
16	1328	1535	11.40	207

TABLE II: A comparison of pixel areas measured algorithmically and by an expert for Fig. 3(a).

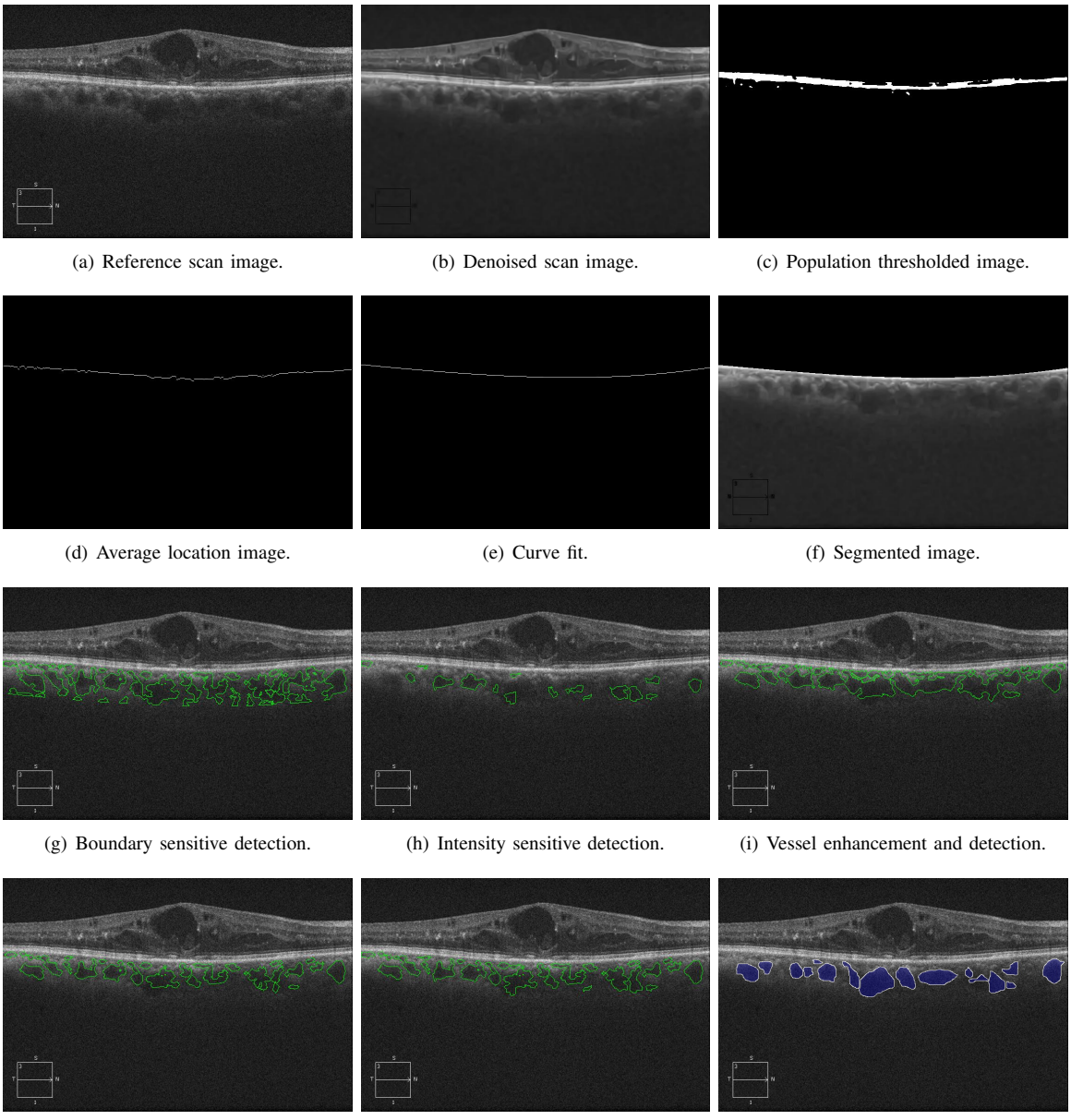

(a) Reference scan image. (b) Denoised scan image. (c) Population thresholded image.

(d) Average location image. (e) Curve fit. (f) Segmented image.

(g) Boundary sensitive detection. (h) Intensity sensitive detection. (i) Vessel enhancement and detection.

(j) Combined boundary sensitive and vessel enhancement. (k) Final contour detection. (l) Ground truth.

Fig. 3: Results of proposed algorithm.